

## SWaP Optimised Parameter Extraction of Radar Signals for Space Electronic Intelligence Application

R.K. Niranjana<sup>#,@,\*</sup>, A.K. Singh<sup>#</sup>, and C.B. Rama Rao<sup>@</sup>

<sup>#</sup>*DRDO-Defence Electronics Research Laboratory, Hyderabad - 500 005, India*  
<sup>@</sup>*Department of ECE, National Institute of Technology, Warangal - 506 004, India*  
<sup>\*</sup>*E-mail: niranjanrk2004@gmail.com*

### ABSTRACT

Space-based electronic intelligence system provides wide coverage and unrestricted access to adversary radar signals. These systems play a vital role in strategic intelligence gathering for assessing electronic order of battle. These systems need to be SWaP optimized with highly efficient algorithms to extract accurate radar parameters. The realization of such a system is a persistent challenge due to the limited availability of space graded components and associated tools. Towards this, the paper deliberates upon various signal processing algorithms to achieve highly accurate direction-of-arrival (DOA), high-frequency resolution and precise timing information for pulse width and pulse repetition frequency extraction. All the proposed algorithms have been implemented, ported and tested on Xilinx Kintex Ultra Scale FPGA KU060 and being evaluated in the radiation setups to establish the performance. High DOA accuracy and frequency accuracy of the order of 0.3 degree and 0.64 MHz respectively have been achieved.

**Keywords:** Interferometry; Electronic intelligence; Direction-of-arrival; Interpolation; Autocorrelation

### NOMENCLATURE

$\theta$	Incident angle
$\psi_{kl}$	First-order virtual phase delay
$\psi_{\delta}$	Second-order virtual phase delay
$f$	Radio frequency
$d$	Antenna separation
$d_{NL}$	Distance between $N$ and $L$ antenna's
$c$	Speed of light
$\lambda$	Wavelength
$\lambda_{\min}$	Wavelength of the highest frequency
$d_{\delta}$	Virtual antenna separation
$m$	Peak frequency bin
$S_f$	Sampling rate
$M$	FFT number of points
$p$	Interpolated peak location
$A_0$	Magnitude of peak bin
$A_1$	Magnitude of previous peak bin
$A_2$	Magnitude of next peak bin

### 1. INTRODUCTION

Surveillance of radar signals is an important operation of electronic warfare (EW). It is having the significance for tactical as well as strategic use to form the electronic order of battle (EOB). In the modern EW scenario, space-based electronic intelligence (ELINT) systems playing a crucial role in gathering information of the global radar threat. They are also having the advantages of very wide coverage and an uninterrupted signal interception. The prime requirement of spaceborne systems is a small size, weight and power (SWaP). The digital techniques meeting the above requirements are preferred in designing

spaceborne ELINT systems. The performance of these systems to be comparable with ground-based ELINT systems<sup>1-3</sup>.

Basic parameters of radar signals are frequency, pulsewidth (PW), power, pulse repetition frequency (PRF) and direction-of-arrival (DOA). To extract the information of radar signals the system configuration with new signal processing algorithms has been proposed.

The DOA of a radar signal is an important parameter because it can't be camouflaged. This parameter can be exploited in many ways which include improving situational awareness, signal sorting or deinterleaving, prompt electronic attack measures (such as jammers) or electronic protection measures (such as chaff) and many more. Accurate DOA measurement is required with available space and resources. There are many contemporary directions finding methods that are suitable for implementation in microwave radar intercept receivers such as rotary direction finding (RDF), amplitude comparison direction finding (ADF), time difference of arrival (TDOA), phase difference of arrival (PDOA) and frequency difference of arrival (FDOA). The PDOA is also known as interferometry<sup>4-5</sup>.

The baseline interferometry (BLI) approach based on four antennas is used to get less DOA error<sup>6-7</sup>. But the system designed using this approach will have more weight because of the requirement of 4 antennae, 4 channel down-conversion, analog-to-digital converters (ADC) and processing blocks. When processing elements are more the power consumption also will be more. Finally, size also increases based on the number of antennae and processing elements. Practically, three different types of antennae are required for coverage of 0.5 GHz to 18 GHz band which requires 12 antennae for

azimuth coverage alone. Similarly, 12 more antennas are required for coverage of elevation. The requirement of hardware increases as per system design.

A virtual antenna based BLI algorithm using three antennae and three-channel receiver are proposed for DOA extraction. The hardware requirement is further optimized with a common master antenna for azimuth and elevation. Measured DOA root-mean-square error (RMSE) using virtual 3 antennae based BLI is more compared to 4 antennae based BLI. This is compensated by using a noise cancellation technique on digitized intermediate frequency (IF) data. Smallest virtual antenna distance also can be increased beyond  $\lambda_{\min}/2$  due to less field-of-view (FOV) requirement of space ELINT system which improves DOA RMSE.

The frequency-domain detection based on FFT itself is frequently used in digital receivers<sup>8</sup>. Frequency extraction is proposed based on the FFT interpolation. Overlapped FFT is used to get the pulse width and pulse repetition interval accuracy advantage. But still, it is difficult to get the advantage equivalent to time-domain processing<sup>9</sup>. Moving autocorrelation algorithm is used to extract pulse repetition interval and pulse width<sup>10</sup>. Emitter identification is effective if parameters are measured accurately<sup>11-12</sup>.

**2. PROPOSED ALGORITHMS**

The space ELINT receiver configuration is shown in Fig. 1. It uses three-antenna array in virtual BLI formation followed by three-channel superhet receiver. Three-channel ADC does the digitization of all three IFs signals which are down-converted by the superhet receiver. In this, various algorithms are applied to extract the pulse descriptor word (PDW) of the signal.

Virtual antenna based BLI algorithm for DOA extraction, FFT based interpolation algorithm for frequency extraction and autocorrelation algorithm for amplitude, PW and PRI extraction are employed. Amplitude is used for pulse detection. All proposed algorithms are described as follows.

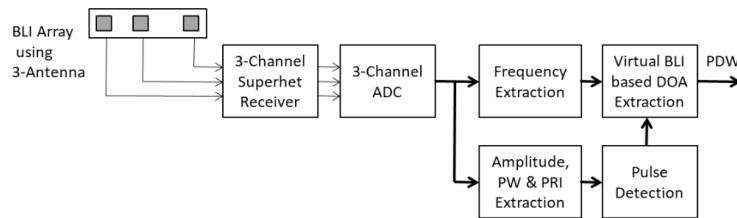


**Figure 1. Space ELINT receiver configuration.**

**2.1 Virtual Antenna based Direction of Arrival Extraction**

One advantage of Interferometry is that very accurate phase measurements can be obtained with digital hardware at a moderate sampling rate and so high accuracy DOA estimate can be obtained with shorter baselines and without the demanding timing constraints. Modern digital Interferometers achieve sub-degree accuracies. Interferometry exploits the propagation phase delay between two spatially alienated antennas to estimate the DOA of a signal. In recent decades, the advent of high-speed analog to digital converter (ADC), high-performance field

programmable gate arrays (FPGAs) and digital computing had led to the development of high fidelity digital receivers. With modern technologies, the implementation of phase-coherent, multi-channel digital receivers have become increasingly more cost-effective. Furthermore, the flexibility of digital computing has allowed the implementation of higher performance algorithms compared to traditional analog counterparts. The interest to use, digital interferometers are increased in recent years to provide fast and accurate DOA estimate for military ES and ELINT systems.

The ELINT receivers are intended to provide early warning to the presence of radars. They are generally positioned at large distances from the radar. The radar signal arriving at the ELINT receiver antenna array can, therefore be reasonably approximated as a uniform plane wave. Here 1, 2, 3 ..., N are the antennas,  $\theta$  is the intercept angle and  $d_{NL}$  are distances between antennas.

The DOA of the signal is estimated as below, by estimating the frequency and phase delay of the signal between the two antennas outputs.

$$\hat{\theta} = \sin^{-1} \left( \frac{\lambda \hat{\psi}}{2\pi d} \right) \tag{1}$$

where wavelength  $\lambda = c / f$ . The baseline of the interferometer is often referred to as antenna separation  $d$ . The accuracy of DOA estimate can be improved by one of the factors such as

- Increasing the SNR of the signal,
- Increasing the signal duration (number of samples),
- Increasing the signal frequency,
- Operating closer to broadside, and
- Increasing the antenna separation.

The first three parameters can be changed by the radar as the parameters of the radar are beyond the control of the ELINT receiver.

Higher baseline Interferometers are designed to achieve higher DF Accuracy. The most popular ambiguity resolution method is based on the Chinese remainder theorem (CRT) and requires appropriately chosen interferometer baselines<sup>13-14</sup>.

For larger aperture, unambiguous DOA estimates can generally be obtained with fewer intermediate baselines than the short baseline ambiguity resolution method. Figure 2(a) describes a simple set of interferometer baselines comprising 4 antennas whereas Fig. 2(b) describes an extended set of interferometer baselines comprising of 4 antennas<sup>15</sup>. The longest baseline  $d_{41}$  provides the best DOA estimation.

DOA accuracy is further increased with more number of baselines i.e. antenna. To process more number of antennas either parallel processing to be carried out that will increase the system hardware and system power or more switching to be done which decreases the probability of intercept (POI) of the radar signal. The effort has been to achieve higher DF accuracy using three channels per Antenna system with certain constraints such as a decrease in FOV and lesser phase margin than earlier configuration and also use of noise cancellation before computing the DOA.

The first constraint is possible to resolve by changing the path of the space vehicle during the predefined mission.

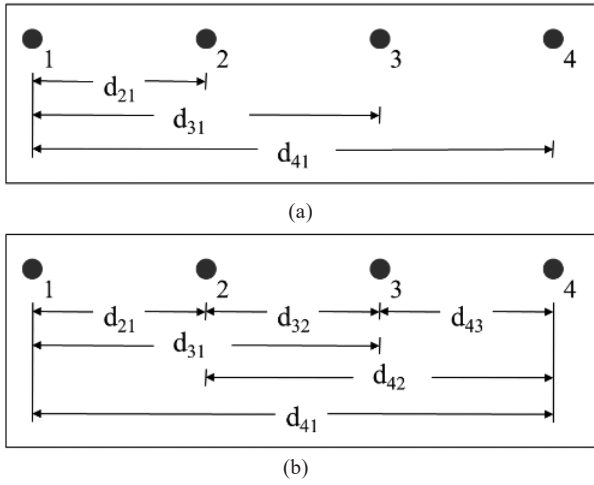


**Figure 2. (a) A simple set of interferometer baselines comprising of 4 antennas and (b) An extended set of interferometer baselines comprising of 4 antennas.**

Whereas the phase errors are minimized by choosing the good hardware component which is reliable for a particular phase margin of the algorithm so that it could not give wrong DOA estimates.

Based on the above constraint, there is an alternative interferometric algorithm Virtual Baseline Interferometer (VBI) which is based on a second-order difference array<sup>16</sup>. This VBI is computationally as fast as a conventional interferometer and also provides unambiguous DOA estimation using two long baselines.

Figure 3(a) describes the concept of the Virtual Baseline Interferometer, where only 3 antennae are required. The ambiguous first-order phase delays for  $d_{21}$  and  $d_{32}$  baselines i.e.  $\psi_{21}$  and  $\psi_{32}$  respectively are derived as below using Eqn (1),

$$\psi_{21} = \frac{2\pi d_{21}}{\lambda} \sin \theta \quad (2)$$

$$\psi_{32} = \frac{2\pi d_{32}}{\lambda} \sin \theta \quad (3)$$

It is assumed that  $d_{32} > d_{21}$  and  $d_{21} \gg \lambda_{\min} / 2$  where  $\lambda_{\min}$  corresponds to the wavelength of the highest frequency of interest. The long baselines suggest that the phase delays are highly ambiguous. The second-order phase delay  $\psi_{\delta}$ , can be calculated as the difference between the first-order delays using Eqns. (2) and (3),

$$\psi_{\delta} = \psi_{32} - \psi_{21} = \frac{2\pi(d_{32} - d_{21})}{\lambda} \sin \theta = \frac{2\pi d_{\delta}}{\lambda} \sin \theta \quad (4)$$

where,  $d_{\delta} = d_{32} - d_{21}$ , this is equivalent to the creation of antennae virtual pair with a baseline of  $d_{\delta}$  as depicted in Fig. 3(b).

This virtual baseline phase delay can be unambiguous provided that the baseline is sufficiently short. It means, that it satisfied the following constraint,  $0 < d_{\delta} \leq \lambda_{\min} / 2$ . The unambiguous estimate of DOA of the signal using the basic interferometer equation is written as

$$\hat{\theta} = \sin^{-1} \left( \frac{\lambda \psi}{2\pi d_{\delta}} \right) \quad (5)$$

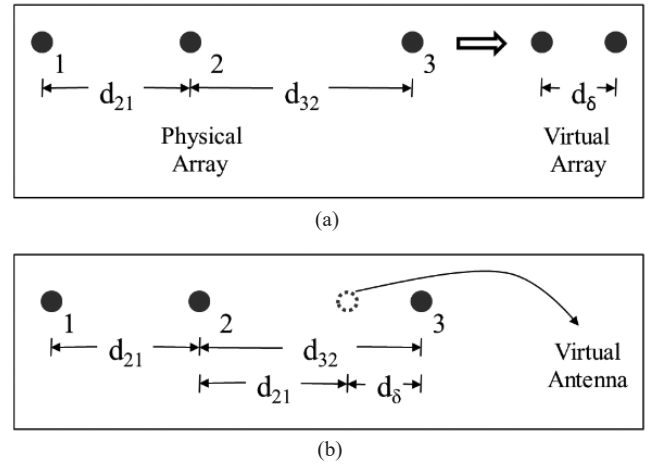


**Figure 3. (a) Virtual baseline interferometer comprising of 3 antennas and (b) Physical interpretation of virtual baseline interferometer.**

The RMS error of the virtual baseline interferometer is expected to be degraded compared to the first-order interferometer with a physical baseline  $d_{\delta}$ . It is attributed to the fact that three antennae outputs are used to estimate the phase delay of a virtual two antenna interferometer. The extra antenna output is expected to introduce more noise to the phase delay estimation and hence lead to a reduction in DOA estimation performance. This error can be reduced by using the longest baseline of the antennas array. The Eqn (5) is limited to a virtual short baseline of  $d_{\delta}$  and does not take advantage of the higher accuracy offered by the longer physical first-order baselines i.e.  $d_{21}$ ,  $d_{32}$ , or  $d_{31}$ . The longest first-order baseline  $d_{31}$  offers an improvement in the DOA estimation by a factor as below:

$$\text{Improvement} = \sqrt{3} * (d_{31} / d_{\delta}) \quad (6)$$

At 6 GHz with  $d_{21} = 45$  mm,  $d_{32} = 52.5$  mm and hence  $d_{31} = 97.5$  mm the DOA RMSE achieved is  $13.7981^{\circ}$  using virtual smallest baseline ( $d_{\delta}$ ). Whereas, DOA RMSE achieved is  $0.6427^{\circ}$  using the longest baseline ( $d_{31}$ ). The factor of improvement using the longest baseline is 21.4679. The theoretical factor of improvement is 22.516 using Eqn. (6). This shows the factor of improvement is approximately matching the theoretical value. The range for 6-18 GHz is  $0.2102^{\circ}$  to  $0.6432^{\circ}$  using 3 antennas. Hence, this method provides comparable results with a less number of antennas, and hence it is an SWaP optimized approach.

## 2.2 Frequency Extraction

Fast Fourier transform (FFT) is used frequently to estimate the frequency of the signal. The FFT number of points is limited due to computational requirements. This restricts the frequency resolution of the FFT. The number of points is selected as a trade-off between the collected data for processing and the frequency resolution or frequency accuracy. The higher FFT number of points provides fine frequency resolution and accuracy which is hardware intensive and consumes more power.

Here Curve Fitting or Interpolation technique has been

used to achieve better frequency accuracy with less FFT number of points<sup>17-22</sup>. The frequency of each component is computed from their respective bin number in the spectrum with a resolution that depends on sample length. If the signal frequency is not the multiple of frequency resolution i.e.  $S_f/M$ , it will not fall on the peak. However, it will distribute near actual frequency and appear on several bins. In this case, the magnitudes of close by bins are used to estimate the actual signal frequency. The curve fitting using interpolation is used to improve the frequency resolution of the measured signal frequency component. Figure 4 shows the FFT frequency response for M points FFT spectrum. The x-axis represents the frequency bin and magnitude is represented by the y-axis. The location of the previous peak bin is represented as  $m-1$ , peak bin as  $m$  and next peak bin as  $m+1$  of the spectrum. The  $A_1$ ,  $A_0$ ,  $A_2$  are the respective magnitudes. The center point at  $p$  in fractional bins gives us an interpolated peak location.

The proposed frequency estimation using the curve fitting interpolation method calculates the offset  $p$  in frequency bin  $m$  using the three maximum amplitude samples for high accuracy frequency estimation of the signal.

The measured course frequency of the signal using FFT spectrum analysis is given as

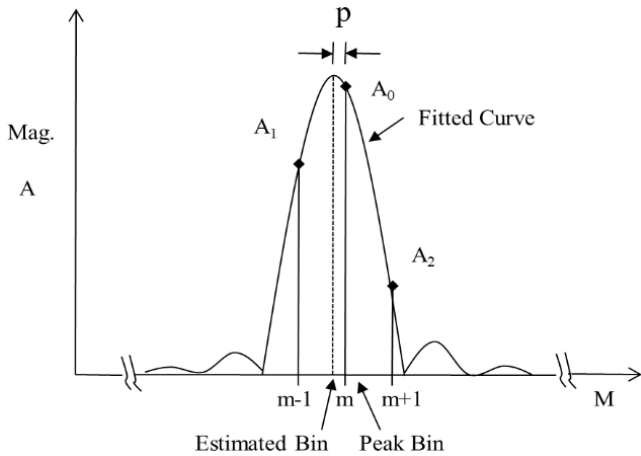


**Figure 4. FFT frequency response with curve fitting interpolation.**

$$\text{Course Frequency} = m * (S_f / M) \quad (7)$$

The frequency bin offset or peak location computed using interpolation is given in bins by

$$p = \frac{(A_1 - A_2)}{2(A_1 + A_2 - 2A_0)} \quad (8)$$

The estimated frequency bin is measured as

$$\text{PeakEstimatedBin} = m \pm p \quad (9)$$

And estimated frequency is measured as

$$\text{FrequencyEstimated} = (m \pm p) * (S_f / M) \quad (10)$$

The sufficient fractional number of bits is to be allocated for  $p$  to get the more advantage of estimation for hardware implementation. Accordingly, the number of bits allocation for  $m$  is also increased.

### 2.3 Pulse width and Time of Arrival Extraction

Measurement of time of arrival (TOA) is a critical parameter of the ELINT system. The accuracy of TOA determines the accuracy of PW and PRF. In the digital domain traditionally, FFT based approach is used to measure this parameter. But the TOA resolution is limited by the FFT size. The autocorrelation approach is used extensively to overcome this limitation. This technique requires in-phase and quadrature-phase data and carries out autocorrelation to find out TOA. The TOA resolution is improved to the order of the basic clock. This technique is optimized towards the least possible resource consumption without compromising the sensitivity and dynamic range of the ELINT system. This approach has been proposed for TOA, PW and PRF measurements<sup>10</sup>.

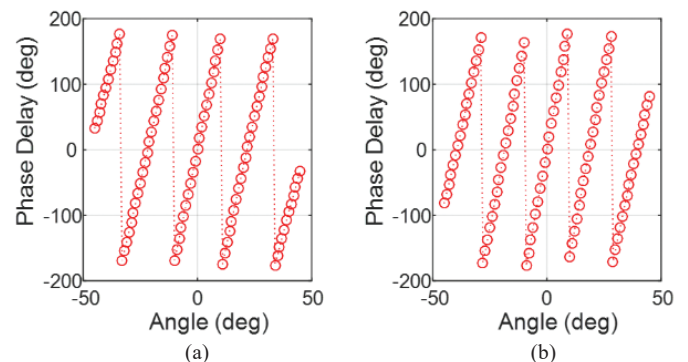
## 3. SIMULATION RESULT AND DISCUSSIONS

Three antennae based BLI algorithm is implemented in Matlab. The first ambiguous phase is converted into an unambiguous phase from the smallest baseline unambiguous phase. Measured AOA error and RMSE are shown for  $\pm 45^\circ$  FOV between 4 antennae and 3 antennae. These results are also generated using an experimental set-up for  $\pm 25^\circ$  FOV. The simulation using noise cancellation technique is given for 3 antennae and comparison is shown without the noise cancellation technique. These results are shown below.

### 3.1 Simulation Result for Direction of Arrival

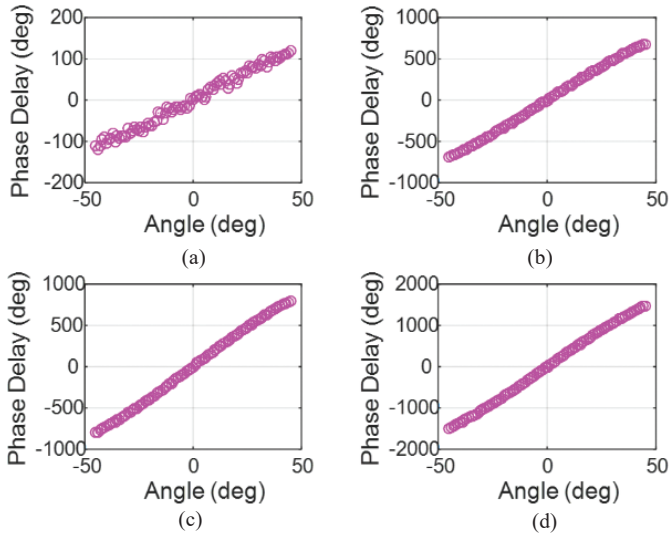
The performance of the virtual baseline interferometer algorithm has been simulated for frequency band 6 - 18 GHz. The spacing between the antennas are  $d_{21} = 45$  mm,  $d_{32} = 52.5$  mm. Using Eqn. (8) the  $d_8 = d_{32} - d_{21} = 7.5$  mm. The distance  $d_{21}$  and  $d_{32}$  are chosen such that  $d_8 < (\lambda_{\min} / 2)$ . The ambiguous phase for the  $d_{21}$  baseline and  $d_{32}$  baseline is shown in Fig. 5. Whereas  $d_8$  which is derived by virtual baseline interferometer, estimates the unambiguous phase shown in Fig. 6.

Figure 7 shows the simulation results for error at 6 GHz between set AOA and measured error and RMSE for 6 GHz to 18 GHz with  $\pm 45^\circ$  FOV. It is evident that the simulation result of 4 antennae is better compared to 3 antennae interferometers. This is obvious as RMSE measured using the smallest physical antenna gives an advantage of  $\sqrt{3}$  times RMSE for the smallest virtual antenna.



**Figure 5. Ambiguous phase for (a)  $d_{21}$  (b)  $d_{32}$  baseline at 18GHz with FOV =  $\pm 45^\circ$ .**





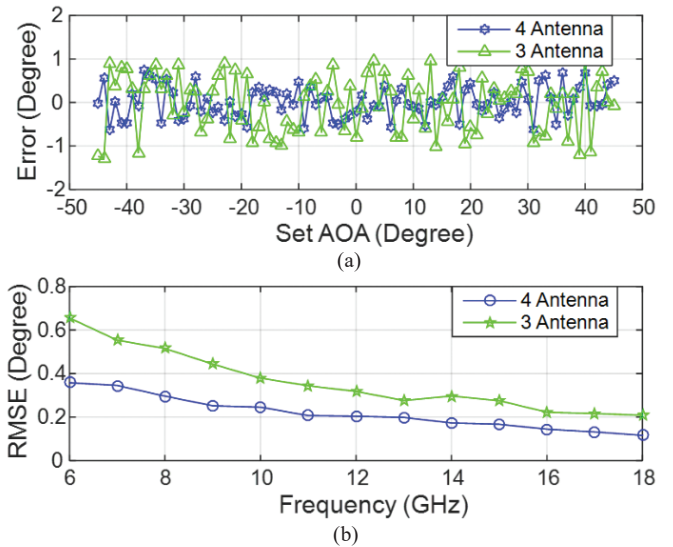
**Figure 6. Unambiguous Phase for (a)  $d_6$  (b)  $d_{21}$  (c)  $d_{32}$  (d)  $d_{31}$  Baseline at 18 GHz with FOV =  $\pm 45^\circ$  using Virtual Baseline Interferometer.**

Figure 8 shows the experimental result generated for  $\pm 25^\circ$  FOV. The phase data is collected in radiation mode. The transmission set-up was kept at a 20 meter distance at the same height as the receiver BLI antennae. The experimental result shows the improvement compared to simulation results as shown in Fig. 7. This is because, the simulation results are generated with a maximum allowable phase error. This performance improvement is attributed to the effects of hardware imperfections for space-qualified components. The experimental result is generated for  $\pm 25^\circ$  FOV which is sufficient for the ELINT system for space application.

Figure 9, shows the experimental result for 3 antenna interferometer with  $\pm 25^\circ$  FOV. This result is generated without and with Noise Cancellation technique<sup>10,23</sup>. The system noise of 200 frames is captured and computed 256 points FFT. This is carried out when input is connected to BITE port and BITE is in signal OFF condition. The estimated average of the noise spectrum is computed for all frames. In system ON condition when input is connected to antenna port and the signal spectrum is computed continuously which is noisy. The estimated noise spectrum is subtracted from the noisy input signal spectrum and an instantaneous magnitude spectrum is computed which is called a restored signal. Again restored time-domain signal is computed by inverse FFT. The SNR of 4 to 5 dB is improved when the signal is passed through this. This result shows that 3 antenna interferometer provides comparable results with 4 antenna interferometer. It shows, on reducing one antenna alone approximately one-fourth of hardware is reduced. Usually, to cover a complete 0.5 to 18 GHz band three different types of antennae are required. With 3 antennas approach, a total of 9 antennae covers complete band instead of 12 antennae. Hence, the further reduction will be there in processing electronics also.

**3.2 Simulation Result for Frequency Extraction**

The simulation for frequency estimation is carried out in MATLAB for 256 points FFT. The sampling frequency



**Figure 7. Simulation result with FOV =  $\pm 45^\circ$  (a) Set AOA vs Error and (b) Frequency vs RMSE.**

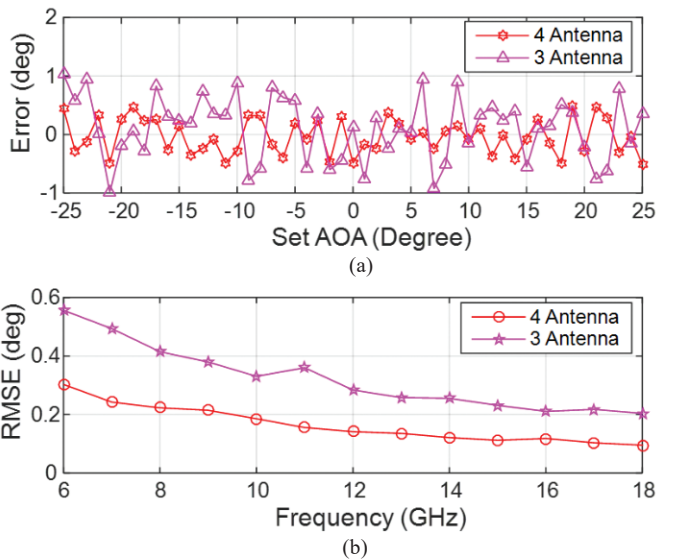


**Figure 8. Experimental result with radiation set-up and FOV =  $\pm 25^\circ$  (a) Set AOA vs error and (b) Frequency vs RMSE.**

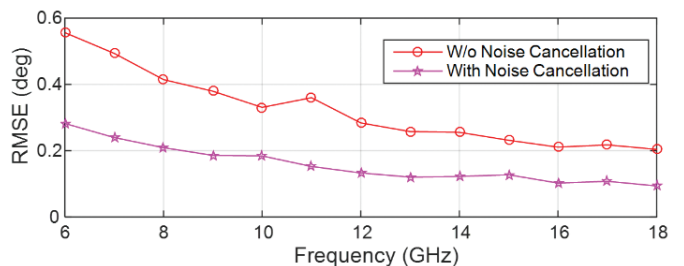


**Figure 9. Experimental result with FOV =  $\pm 25^\circ$  for 3 antenna.**

for bandpass sampling of ADC is chosen as 1.333 GHz. The performance is validated for various power levels and pulse widths. The step size of 0.5 MHz is chosen to vary the frequency of the input signal and frequency measurement RMS error is

calculated. The input frequency of 1200 MHz and a pulse width of 200 ns are chosen for MATLAB simulation. The measured frequency error is 2.3828 MHz using normal FFT analysis whereas, the measured frequency error is 0.5218 MHz using the frequency estimation algorithm.

Figure 10 shows the MATLAB simulation output of 256 points FFT. The measurement frequency RMS error is computed in this simulation for the frequency range of 1200 to 1220 MHz. The measured frequency RMS error is 1.4905 MHz and peak frequency error is 2.5313 MHz using normal FFT analysis. Whereas, the measured frequency RMS error is 0.6399 MHz and peak frequency error is 0.9179 MHz using the frequency estimation algorithm.

**4. FPGA IMPLEMENTATION**

Three antennae based baseline interferometry and frequency estimation approach is implemented in field-programmable gate array (FPGA) using Xilinx system generator. The system generator design is given in Fig. 11. FFT of 256 points is computed on all three channels and phase is computed. The phase difference is computed using the phase of each channel and DOA is measured. In one of the channel frequency interpolation is implemented. The detection is carried out on the instantaneous amplitude profile which is computed from the same antenna channel. The PRI and PW are also computed using the instantaneous amplitude profile.

The design is implemented on the Xilinx Kintex Ultra Scale FPGA XCKU060-FFVA1517 which is footprint compatible with radiation tolerant device XQRKU060-CNA1509. The resources are compared with the four antennae based BLI approach and mentioned in Table 1.

**Table 1. Resource comparison (Xilinx FPGA: XCKU060-FFVA1517)**

FPGA resource utilisation	3 Antenna based proposed approach	4 Antenna based approach	Savings in %
Registers	16567	21355	22.4
LUTs	12893	16283	20.81
36 Kb Block RAM	757	1026	26.21
18 Kb Block RAM	1532	2042	25.02
DSP48 Slices	40	50	20.0
Total Power (mW)	16464	21152	22.16

**5. CONCLUSIONS**

It is evident from proposed approaches that there is an improvement in resolution and accuracy of measurement for various parameters direction-of-arrival, frequency etc. with fewer hardware resources. In case of direction finding, less number of front ends and antennas combinations can be realizable in the system that provide RMS DOA error of less than 0.3 degree with less weight and small size which is the requirement of space platform. The frequency measurement accuracies achieved is less than 0.6399 MHz RMS with this approach against 1.4905 MHz RMS with simple FFT spectrum analysis using 256 points FFT. The autocorrelation

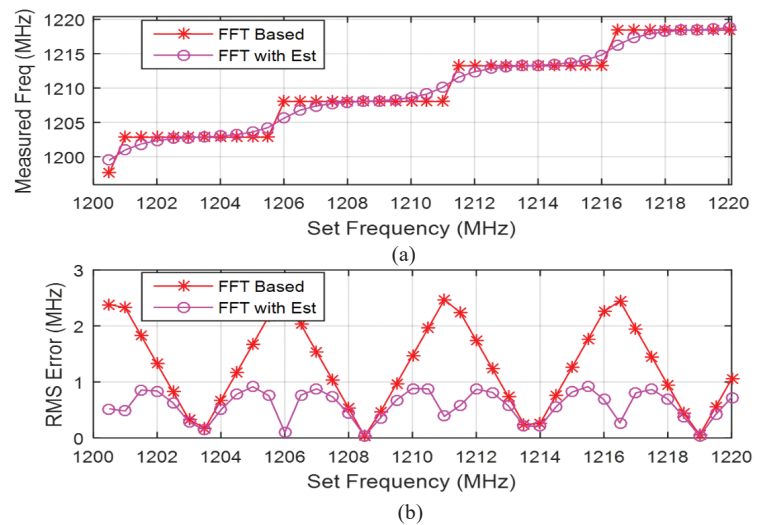


**Figure 10. (a) Set Frequency vs Measured Freq (b) Set Frequency vs RMS Error for 256 Points FFT.**

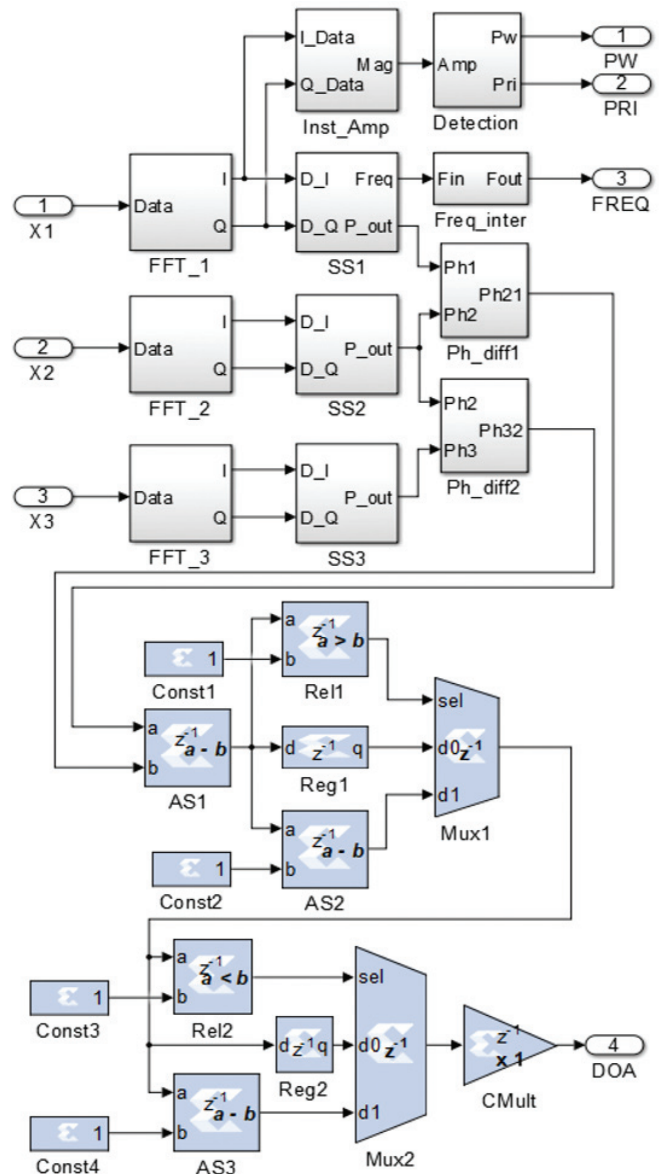


**Figure 11. System generator design.**

with FFT combination approach improves the PW and TOA measurements that can be measured with high accuracy with very few resources. It also helps to reduce the power consumption which is high in today's system.

Apart from the measurement of the basic parameters, there is more scope in the future to measure the more complicated parameters like intra-pulse modulation parameters information of radar. These measurement techniques will be helpful for realizing a better ELINT system based on a digital receiver for space applications.

## REFERENCES

1. Adamy, D.L. EW 101: A first course in electronic warfare. Boston, MA, USA: Artech House, 2001.
2. Adamy, D.L. EW 102: A second course in electronic warfare. Boston, MA, USA: Artech House, 2004.
3. Lyons, R.G. Understanding digital signal processing. Boston, Addison Wesley Longman, Inc., 1997.
4. Wiley, R.G. ELINT: The interception and analysis of radar signals. Artech House Radar Library, Artech House, Inc., 2006.
5. Lipsky, S.E. Microwave passive direction finding. SciTech Publishing, Inc. 2004.
6. Orduyilmaz, A.; Kara, G.; Gürel, A.E.; Serin, M.; Yildirim, A. & Soysal, G. Real time four channel phase comparison direction finding method. *In Proceedings of the Signal Processing and Communications Applications Conference (SIU), Izmir, Turkey, 2018.* doi: 10.1109/SIU.2018.8404590
7. Gürel, A.E.; Orduyilmaz, A.; Yıldırım, S.A.; Kara, G.; Serin, M.; Ortatatlı, I.E. & Yildirim, A. Real time passive direction finding in FPGA environment. *In Proceedings of the Signal Processing and Telecommunication Applications, IEEE, Antalya, 2017.* doi: 10.1109/SIU.2017.7960593
8. Singh, A.K. & Rao, S.K. Digital receiver-based electronic intelligence system configuration for the detection and identification of intrapulse modulated radar signals. *Def. Sci. J.*, 2014, **64**(2), 152-158. doi:10.14429/dsj.64.5091
9. Niranjan, R.K. & Bhukya, R.N. Approach of Pulse parameters measurement using digital IQ method. *IJIEE*, 2014, **4**(1), 31-35. doi: 10.7763/IJIEE.2014.V4.403
10. Niranjan, R.K.; Singh, A.K. & Rama Rao, C.B. High accuracy parameter estimation for advanced radar identification of electronic intelligence system. *Def. Sci. J.*, 2020, **70**(3), 278-284. doi: 10.14429/dsj.70.15105
11. Gupta, M.; Hareesh, G. & Mahla, A.K. Electronic warfare: issues and challenges for emitter classification. *Def. Sci. J.*, 2011, **61**(3), 228-234. doi: 10.14429/dsj.61.529
12. Conning, M. & Potgieter, F. Analysis of measured radar data for specific emitter identification. *In Proceedings of the Radar Conference, IEEE, Washington, DC, USA; 2010.* doi: 10.1109/RADAR.2010.5494658
13. Xia, X.G. & Wang, G. Phase unwrapping and a robust Chinese remainder theorem. *Signal Proces. Lett.*, 2007, **14**, 247-250.
14. Sundaram, K.R.; Mallik, R.K. & Murthy, U.M.S. Modulo conversion method for estimating the direction of arrival. *IEEE Trans. Aerospace Electron. Sys.*, 2000, **36**(4), 1391-1396. doi: 10.1109/7.892687
15. Wu, Y.W.; Rhodes, S. & Satorius, E.H. Direction of arrival estimation via extended phase interferometry. *IEEE Trans. Aerospace Electron. Sys.*, 1995, **31**(1), 375-81. doi: 10.1109/7.366318
16. Peter, Q.C. Ly; Stephen, D.E.; Douglas, A. G. & Joy, Li. Unambiguous AOA Estimation Using SODA Interferometry for Electronic Surveillance. *In Proceedings of the Sensor Array and Multichannel Signal Processing Workshop (SAM), IEEE, Hoboken, NJ, USA.* doi: 10.1109/SAM.2012.6250488.
17. Tsui, J.B.Y. Digital techniques for wideband receivers. 2nd Ed, Norwood, MA Artech House, 2004.
18. Akima, H. A method of smooth curve fitting. ESSA Tech, ERL 101-ITS 73 US Government Printing Office, Washington, D.C., Jan. 1969.
19. Quinn, B.G. Estimating frequency by interpolation using Fourier coefficients. *IEEE Trans. Signal Processing*, 2014, **42**(5), 1264-1268. doi: 10.1109/78.295186
20. Voglewede, P. Parabola approximation for peak determination. *Global DSP Magazine*. 2004, **3**(5), 13-17.
21. Helton, J.; Henry, C.I.; David, M.L. & Tsui, J.B.Y. FPGA- Based 1.2 GHz Bandwidth digital instantaneous frequency measurement receiver. *In Proceedings of ISQED. San Jose, CA, USA, 2008.* 265-270. doi: 10.1109/ISQED.2008.4479798
22. Djukanovi, S. An accurate method for frequency estimation of a real sinusoid. *In Proceedings of the Signal Processing Letters, IEEE, 2016,* **23**(7). doi: 10.1109/LSP.2016.2564102
23. Saeed, V. Advanced digital signal processing and noise reduction. 4th Ed., John Wiley & Sons, 2008, pp. 321-323.

## ACKNOWLEDGMENTS

It is immense pleasure to thank Director DLRL, Additional Director and Wing Head for their continuous guidance and support toward this activity. The authors are also would like to thanks anonymous reviewers for making various useful suggestions and comments.

## CONTRIBUTORS

**Mr R.K. Niranjan** received his BE (ECE) from Dr Hari Singh Gour University, Sagar, in 1998 and ME (Systems and Signal Processing) from Osmania University, Hyderabad, in 2012. Currently pursuing his PhD from NIT, Warangal. Presently working as Scientist 'F' at DRDO-Defence Electronics Research Laboratory, Hyderabad. He has been working in the area of signal processing for electronic warfare systems with specific interests in the area of data acquisitions and DSP algorithms implementations in FPGA for real time applications.

In the current study, he conceived the concept, carried out the literature survey and complete experimental work with interpretation and analysis of result.

**Dr A.K. Singh**, did ME in Digital System (ECE) and PhD from Osmania University, in 2003 and 2015, respectively. Currently working as Scientist 'G' at DRDO-Defence Electronics Research Laboratory. He was the instrumental in design and development of digital receiver. His area of interest includes high-speed board design, time-frequency signal processing, and EW Receiver design. Presently he is working for space systems design.

In the current study, he has supported in making experimental setup, reviewed the incremental work and provided various valuable inputs.

**Prof. C.B. Rama Rao**, did his post-graduation from JNTU, Kakinada and PhD from IIT, Kharagpur. He has been currently working as Professor in the Department of Electronics and Communication Engineering, NIT Warangal, India. His research interests primarily include adaptive signal processing, musical instrumental signal processing, speech signal processing and biomedical signal processing. He has published more than 32 papers in reputed Journals and Conferences.

In the current study, he has given the idea, reviewed the work, validated the results, continuously provided the guidance and given many valuable inputs.